IFAC Conference on Advances in PID Control
PID'12
Brescia (Italy), March 28-30, 2012

An approach for calculating all stable PID parameters for time delay systems with uncertain parameters

Frank Schrödel, Jan Maschuw, Dirk Abel

Institute of Automatic Control, RWTH Aachen University,
52074 Aachen, Germany,
e-mail: {F.Schroedel, J.Maschuw, D.Abel}@irt.rwth-aachen.de

Abstract:
There exists a large number of PID tuning rules for LTI systems. However, these rules often use time delay approximations and ignore parameter uncertainties. This work updates the classical parameter space approach to an one step PID tuning approach to guarantee robust stability for LTI time delay systems with explicit consideration of uncertainties in the plant parameters and the time delay. The basic idea is to calculate how the root boundaries changes due variation of system parameters. Bands of root boundaries are determined by this analysis. The challenging task of robust stability of time delay systems is converted to an easier minimum/maximum search to estimate the borders of the root boundary bands. The presented method satisfies robust stability with only small conservatism.

Keywords: PID control, time delay, robust control, parameter space.

1. INTRODUCTION

The stability analysis of time delay systems, especially with uncertain and immeasurable time delay is a very difficult task. A wide range of approaches exists to estimate the stability of LTI time delay systems. They are based on e.g. Lyapunov-Krasovskii (Gu and Niculescu (2003)), Lyapunov-Razumikhin (Gu and Niculescu (2003)), the direct method (Walton and Marshall (1987)) and the Rekasius method (Ebenbauer and Allgöwer (2006)). These approaches are often very challenging, conservative and do not support parameter uncertainties directly.

The goal of the presented approach is to calculate the whole space of stabilizing PID parameters based on the system parameters and their corresponding range of uncertainty. The presented approach to guarantee robust stability is based on the classical parameter space approach by Ackermann (2002). Hohenbichler and Abel (2009) extends this approach to deal in the synthesis step with time delay systems. But the application to robust stability and the performance conditions were not addressed. Also, the analysis step was not developed.

These outstanding analyses should be rescheduled in the present paper. The following method updates the classical parameter space approach to a one step approach to guarantee robust stability. To realize this, it is studied how the root boundaries shift when the plant parameters vary with respect to the uncertainties. Based on this, a worst case estimation is developed and bands of root boundaries result. As will be shown in the following, the highly challenging problem to guarantee robust stability can be converted to a simple minimum/maximum estimation to calculate the borders of the of root boundary bands. With this approach, the second step of the classical parameter space approach is automatically verified. Consequently, in only one step a necessary and for a wide class of systems sufficient (with only small conservatism) region of robust stability for the PID parameters can be derived.

The structure of this paper is as follows. In the second section, the basics of the classical two step parameter space approach are repeated and the following used method is sketched to modify this classical approach to a one step approach for guaranteed robust stability. In the next section, the CRB calculation for the delay-free case is presented. Following this, an extension of this approach (for the delay case) is demonstrated. In the fifth section, the resulting stable PID space is discussed to illustrates the results of the presented approach. The sixth section deals with a short overview of the planned and partially implemented methods to realize performance requirements with respect to the previously calculated PID space. The paper ends up with a conclusion.

2. MAIN IDEA OF THE ROBUST APPROACH

The classical parameter space approach consists of two steps. In the first step (synthesis), the stable 3D region in the PID controller parameter space ($\boldsymbol{k}$) is calculated for one fixed system parameter combination ($A(s)$, $R(s)$, L). Based on this, in the second step (analysis), it is verified that (with respect to the system parameter uncertainty ($\boldsymbol{q}$)) every parameter combination of the previously calculated PID space leads to a stable closed loop system.

To calculate the PID parameter space, the following nomenclature is used. The PID controller has the form

$$PID(s, \boldsymbol{k}) = \frac{K_I + K_P s + K_D s^2}{s} \tag{1}$$

and the LTI time delay systems has the transfer function $G(s) = \frac{A(s)}{R(s)} e^{-Ls}$. For the following stability analysis, the location of the eigenvalues are calculated based on the characteristic equation of $G(S)$. This leads to the quasi polynomial

$$P(s, \boldsymbol{k}, L, \boldsymbol{q}) = \left(K_I + K_P s + K_D s^2\right) A(s, \boldsymbol{q}) + \underbrace{s R(s, \boldsymbol{q})}_{B(s, \boldsymbol{q})} e^{sL} \quad (2)$$

with the polynomials

$$A(s, \boldsymbol{q}) = a_0(\boldsymbol{q}) + \ldots + a_m(\boldsymbol{q}) s^m, \qquad a_m(\boldsymbol{q}) \neq 0 \quad (3)$$

and

$$B(s, \boldsymbol{q}) = b_0(\boldsymbol{q}) + \ldots + b_n(\boldsymbol{q}) s^n, \qquad b_n(\boldsymbol{q}) \neq 0. \quad (4)$$

The parameter uncertainty can be graphically represented by the Q-box. Fig. 1 illustrates the Q-box of a system with two parameters with two independent lower (q_i^-) and upper (q_i^+) bounds respectively. The dimension of the Q-box corresponds to the number of uncertain system parameters. The goal of the parameter space approach is to find all PID parameters which guarantee for the whole system parameter family (described by the Q-box) a stable closed loop behavior.

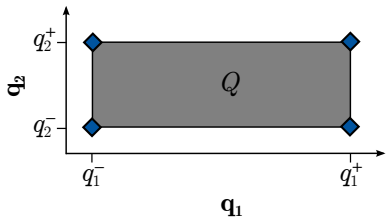

Fig. 1. Parameter uncertainty area

The starting point of the classical synthesis step is the Hurwitz stability. The borders which limit the PID parameter space (root boundaries) can be calculated with respect to the border crossing rate. The root boundaries can be interpreted as equations to calculate those PID parameter combinations that lead to leave the stable left-half s-plane. The present approach starts like the classical parameter space approach with the calculation of the borders of the PID parameter space based on Hohenbichler and Abel (2009). In addition, it is studied how the root boundaries shift when the plant parameters vary. This leads to the following worst case analysis of all three types of root boundaries.

2.1 Real root boundary (RRB)

The RRB is the root boundary for the case when the roots of the system leave the left-half s-plane by crossing the imaginary axis along the real axis. To calculate the RRB, $s = 0$ must be inserted into the quasi polynomial equation (2). This follows $P(s = 0, \boldsymbol{k}) = K_I A(0) + B(0) = 0$ and leads to

$$K_I = -\frac{b_0}{a_0}. \quad (5)$$

In case of a PID controller, it holds that $b_0 = 0$, because of the integral part of the controller in equation (2). Thereby, the RRB is simplified to $K_I = 0$, independent of the plant parameters. Hence, this border lies for any system parameter combination at the same value, $K_I = 0$.

2.2 Imaginary root boundaries (IRB)

The second type of root boundaries are the IRBs. Here, the system poles leave the left-half s-plane when the absolute value of s goes to infinity. After inserting $|s| \to \infty$ into equation (2), it holds

$$K_D = \pm \frac{b_n}{a_m}. \quad (6)$$

It is easy to see that equation (6) applies only for systems with the order $n = 2 + m$. The following study is restricted to this class of systems. The two IRB boundaries are directly dependent on the plant parameters. The highest value of K_D from equation (6) results when the highest value of b_n and the smallest of a_m are used. The estimation of the smallest value of K_D is the inverse case. Hence, it is easy to estimate the two worst case IRB bands with consideration of the uncertain system parameters.

2.3 Complex root boundaries (CRB)

The third type of root boundaries are the CRBs. In this case, the system poles cross the imaginary axis with a complex conjugate pole pair. The derivation of the CRB equations is described in detail in Ackermann (2002). Based on this, the c linear (with respect to K_D) CRBs $K_{I,i}$, $i = 1, \ldots, c$ can be calculated as

$$K_{I,i} = \omega_{g,i}^2 K_D + K_{I,i}^0(\omega_{g,i}) \quad (7)$$

with

$$K_{I,i}^0(\omega_{g,i}) = \frac{-R_B \cos(\omega_{g,i} L) + I_B \sin(\omega_{g,i} L) + \omega_{g,i} K_P I_A}{R_A}. \quad (8)$$

R_X represents the real part and I_X the imaginary part of the polynomial X. Keep in mind that R_X and I_X are functions of $\omega_{g,i}$, (see equation (3) and (4)). The singular frequencies $\boldsymbol{\omega_g} = [\omega_{g,1}, \ldots \omega_{g,n}]^T$ are the zeros of

$$0 = \frac{I_A R_B \cos(\omega L) - I_A I_B \sin(\omega L)}{\omega (R_A^2 + I_A^2)} - \frac{R_A R_B \sin(\omega L) + R_A I_B \cos(\omega L)}{\omega (R_A^2 + I_A^2)} - K_P. \quad (9)$$

In the case of parameter uncertainties, the zeros $\boldsymbol{\omega_g}$ of equation (9) are shifted (see section 4). Hence, intervals of each zero $\omega_{g,i}$ results. Whereby a CRB band results for each zero $\boldsymbol{\omega_g}$ interval. A worst case estimation to calculate the bounds of the CRB bands is not as easy as in the case of IRBs. Section 3 and 4 presents some approaches to calculate a worst case estimation of the CRBs boundaries. In the present section, only the basic principle behind the following worst case analysis of the CRBs should be described. The overall idea of the CRB worst case estimation is to find the borders of the CRB bands with respect to the parameter uncertainty. To reduce the computational effort and to simplify the geometric shape of the resulting CRB bands (see Fig. 2) for the subsequent analysis, these optimization task is divided into two sequentially solved problems. Firstly an estimate of the min/max slope ($\omega_{g,i}^2$) of each CRB band (for every zero $\boldsymbol{\omega_g}$ interval) with respect to the uncertainty is done. Based on the min/max $\omega_{g,i}$ of each zero $\boldsymbol{\omega_g}$ interval and the parameter uncertainty, an estimate of the min/max corresponding intersection point ($K_{I,i}^0$) of each CRB band is performed. The optimization strategies for $\boldsymbol{\omega_g}$ and $\boldsymbol{K_I^0}$ are described in detail in section 3 and 4.

In the present approach it is assumed that the bounds (min/max $\omega_{g,i}$) of each zero $\boldsymbol{\omega_g}$ interval generate the min/max $K^0_{I,i}$. But this is not generally fulfilled and generates an overestimation of the CRB bands. Fortunately, the overestimation produces mostly only a small error. The maximum occurring error (shift of the CRB) corresponds to the maximum amount of $K^0_{I,i}$. The amount of $K^0_{I,i}$ is proportional to the amount of $\omega_{g,i}$. In the delay-free case, this amount is very small (see section 3). In the time delay case, the amount of $\omega_{g,i}$ is growing directly with the amount of uncertainty in the time delay L. Therefore it is very easy to quantify and evaluate the conservatism. But above all it should be noted that due to the overestimation, only the areas of the 3D PID space which are located very close to the instability boundaries are lost. An example of the resulting overestimation can be seen in Fig. 2. To create this plot, the example system $G_1(s) = \frac{5s+6}{1s^3+2s^2+7s+5}$ with an ± 10 % uncertainty in all system parameters and in the time delay is used. Fig. 2 illustrates the CRB band (for the first zero $\boldsymbol{\omega_g}$ range) with consideration of parameter uncertainties. For the illustration of the correct solution 10 example CRBs (with different system parameters with respect to the uncertainty bound) were given.

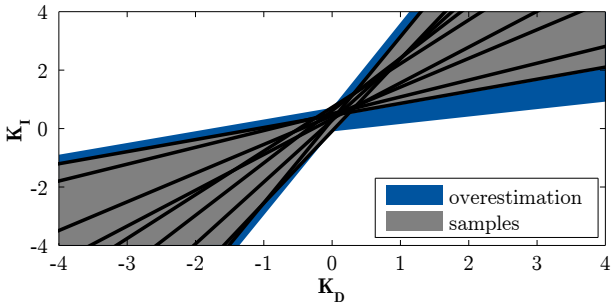

Fig. 2. Overestimation of the CRB bands

3. CRB FOR UNCERTAIN DELAY-FREE SYSTEMS

The following sections demonstrates how a worst case estimate for the CRBs can be exactly realized. At first, the delay-free case is discussed. For this worst case estimate, the borders of the CRBs must be calculated. In order to do so, equations (8) and (9) must be analyzed. Both equations are simplified in the delay-free case ($L = 0$)

$$K^0_{I,i}(\omega_{g,i}) = \frac{\omega_{g,i} K_P I_A - R_B}{R_A} \tag{10}$$

and

$$0 = \underbrace{\frac{I_A R_B - R_A I_B}{\omega(R_A^2 + I_A^2)}}_{g(\omega)} - K_P. \tag{11}$$

The first step is to estimate the borders of each zero $\boldsymbol{\omega_g}$ interval and so for each CRB band. Hence, the min/max zero $\omega_{g,i}$ of each interval of equation (11) must be calculated. The optimization task is formulated in the form

$$\begin{aligned} \min_{\boldsymbol{q}\in Q} \,/\, \max_{\boldsymbol{q}\in Q} \quad & \omega_{g,i} \\ \text{s.t.} \quad & 0 = g(\omega, \boldsymbol{q}) - K_P. \end{aligned} \tag{12}$$

It can be seen that this problem is not convex. There exist some very powerful numeric tools to find the min/max of high dimensional non convex functions (e.g. MATLAB Global Optimization Toolbox). But this numeric tools cannot guarantee to find the global optimum, and hence the correct borders in the parameter space. So, an approach to guarantee the convergence to the global optimum must be developed. The starting point of this approach is to convert the zero search of equation (11) to a min/max search of $g(\omega)$. In Fig. 3 can be seen that the min/max of $g(\omega)$ corresponds to the min/max of $\omega_{g,i}$. To create this plot, the high order nonminimum phase example system from the parameter space section of Ackermann (2002) is used, $G_2(s) = \frac{-s^4-7s^3-2s+1}{1s^6+11s^5+46s^4+95s^3+109s^2+74s+24}$. In Fig. 3 the value of the function $g(\omega)$ was increased and decreased by 50 percent to illustrate the effect on the zeros ω.

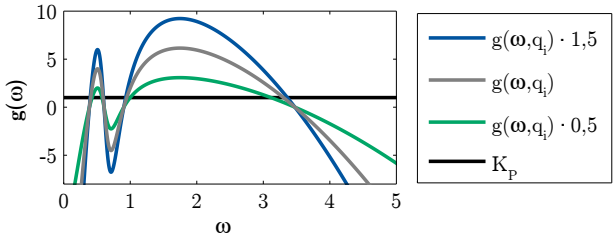

Fig. 3. Relation of the amplitude and the zeros of $g(\omega)$

To find the min/max of $g(\omega)$, the min/max denominator and numerator of $g(\omega)$ must be found. This optimization problem is also non convex. One way to guarantee the convergence is an overestimation. That is demonstrated by the min/max denominator search in the following. To find the maximal denominator, the absolute value of R_A and I_A must be maximal. Based on equation (3) R_A and I_A can be written as a function of ω

$$\begin{aligned} R_A(j\omega) &= a_0 \quad - a_2\omega^2 \; + a_4\omega^4 \; - a_6\omega^6 \; + \ldots \\ I_A(j\omega) &= a_1 j\omega - a_3 j\omega^3 + a_5 j\omega^5 - a_7 j\omega^7 + \ldots . \end{aligned} \tag{13}$$

If all coefficients of the $A(s)$ polynomial are positive, R_A becomes maximum for the maximal values of $[a_0, a_4, a_8, \ldots]$ and the minimal values of $[a_2, a_6, a_{10}, \ldots]$. When a coefficient of $A(s)$ is negative, the opposite bound must be chosen for this coefficient. The only restriction is that $A(s)$ must be an interval polynomial whose coefficients do not change their sign with respect to the uncertainty bounds. The I_A optimization is analogous to the R_A case. The optimization of the individual real and imaginary parts, coupled with the appropriate case distinctions must be applied analogously for the numerator. Hence, the variables in equation (11) are analyzed independently and the resulting optimization problem is easy to solve. The described analyses can also be performed automatically. To do so, all real and imaginary parts are regarded as independent variables that are optimized one by one.

The optimization of equation (10) can be performed similarly. Hence, it is easy to estimate the min/max $K^0_{I,i}$ with the previously calculated min/max $\omega_{g,i}$ of each zero $\boldsymbol{\omega_g}$ interval. From equation (10) and (13) it can be seen that the min/max $K^0_{I,i}$ lie in the corners of the Q-box. For the case of two parameters this result complies with the Kharitonov polynomial theorem. This theorem states that a polynomial of the form $p(s) = a_0 + a_1 s + \ldots + a_r s^r$ with uncertain parameters $a_u^- \le a_u \le a_u^+$ for $u = 0, \ldots, r$ is stable if and only if the following four polynomials are stable (by Kharitonov (1978))

$$\begin{aligned} p_1(s) &= a_0^- + a_1^- s + a_2^+ s^2 + a_3^+ s^3 + a_4^- s^4 + \dots \\ p_2(s) &= a_0^+ + a_1^+ s + a_2^- s^2 + a_3^- s^3 + a_4^+ s^4 + \dots \\ p_3(s) &= a_0^+ + a_1^- s + a_2^- s^2 + a_3^+ s^3 + a_4^+ s^4 + \dots \\ p_4(s) &= a_0^- + a_1^+ s + a_2^+ s^2 + a_3^- s^3 + a_4^- s^4 + \dots \end{aligned} \tag{14}$$

In the case of two uncertain parameters, the corners of the Q-box (Fig. 1) must be stable. So it can be deduced that an easy way to solve the robust stability problem in the delay-free case (without the conservative optimization) is to plot the PID space of each corner of the Q-box. The intersecting area of the resulting four 3D areas is the stable PID-parameter area for the whole parameter set.

But the Kharitonov polynomial theorem is only valid for interval polynomials. For a polynomial of the form $p(s) = a_0(\boldsymbol{q}) + a_1(\boldsymbol{q})s + \ldots + a_r(\boldsymbol{q})s^r$ with the uncertainly $\boldsymbol{q} = [q_1 \ldots q_k] : q_u^- \leq q_u \leq q_u^+$ for $u = 0, \ldots, r$ the edge theorem must be used (see Fu et al. (1989a) and Fu et al. (1989b)). One approach to transfer this problem in the previously described form is to neglect the $\boldsymbol{q}$ dependency. This transfer (calculation of the limits of each coefficient) is possible without any further effort, but it makes the solution very conservative because of the inherent loss of information. If this problem should be solved with the intersecting area plot approach, the PID space of each parameter combination of the edge of the Q-box must be plotted. With respect to feasibility, this is not applicable because the resulting test set is infinite. In such a case alternative stability analysis methods demonstrated in Fu et al. (1989a) can be applied (even for time delay systems).

4. CRB FOR UNCERTAIN TIME DELAY SYSTEMS

For better understanding, important results are demonstrated by the example system $G_3(s) = G_2(s)e^{-0.75s}$ with a ± 10 % uncertainty in all system parameters and in the time delay. During the following calculation a constant $K_P = 1$ is used. Generally it can be found out, if a system has a time delay, a finite test set (like the Kharitonov polynomials) to use the intersection area approach cannot be found. The reason is the pole movement of such a system. The poles do not move linearly in the s-plane under variation of the time delay L. This phenomena can also be studied in equation (8). This equation shows that the extreme values of $K_{I,1}^0$ are not correlated with the min/max value of the time delay L (vertices of the Q-box), because of the trigometric functions. Hence, in this case it is not sufficient to test only the vertices of the Q-box, which would lead to a finite test set.

Therefore the worst case estimation must be done by using the previously presented optimization method. Like in the delay-free case, this problem is divided into two separate tasks. At first, the min/max $\omega_{g,i}$ for each zero $\boldsymbol{\omega_g}$ interval is found. In the second step, the min/max $K_{I,i}^0$ with the previously calculated min/max $\omega_{g,i}$ is found. Using addition theorems, equation (8) and (9) can be modified to a more convenient form

$$K_{I,i}^0(\omega_{g,i}) = \operatorname{sgn}(I_B) \underbrace{\frac{\sqrt{R_B^2 + I_B^2}}{R_A}}_{\alpha} \sin\left(\omega_{g,i} L + \underbrace{\arctan\left(\frac{R_B}{I_B}\right)}_{\beta}\right) + \underbrace{\frac{\omega_{g,i} K_P I_A}{R_A}}_{\gamma} \tag{15}$$

and

$$0 = \underbrace{\operatorname{sgn}(I_B) \underbrace{\sqrt{\frac{R_B^2 + I_B^2}{\omega^2 \left(R_A^2 + I_A^2\right)}}}_{\delta} \sin\left(\omega L + \underbrace{\arctan\left(\frac{f_2}{f_1}\right)}_{\epsilon}\right)}_{h(\omega)} - K_P \tag{16}$$

with

$$\begin{aligned} f_1 &= I_A I_B + R_A R_B \\ f_2 &= R_A I_B - I_A R_B. \end{aligned} \tag{17}$$

A way to guarantee stability of the resulting PID space (without convergence problems) is an overestimation of equation (16). The idea is to analyze all terms (L, ϵ and δ) in equation (16) separately, like in section 3. The time delay L has the strongest influence on $\boldsymbol{\omega_g}$ because the main cause of the frequency change is based on the time delay variation ΔL (see equation (16) and Fig. 4). But fortunately, the value of the time delay to minimize/maximize $h(\omega)$ is known exactly. $L_{\min}/L_{\max}$ corresponds to $h_{\min}(\omega_g)/h_{\max}(\omega_g)$ and leads so to the min/max $\omega_{g,i}$. Hence, it can be assumed that uncertainty in the time delay does not produce conservatism. The term ϵ changes the frequency of $h(\omega_g)$ in equation (16). It is easy to see that ϵ becomes maximal when f_1 is minimal and f_2 maximal. An increase in δ causes an growth of the amplitude of $h(\omega_g)$ in equation (16) and the zeros $\boldsymbol{\omega_g}$ are shifted outwards. The largest amplitude results in the largest absolute value of R_A and I_B as well as the smallest possible absolute value of R_A and I_A. Hence, every real and imaginary part in equation (16) and (17) must be optimized separately, like in section 3. So, the smallest/largest zero of equation (16) can easily be calculated, because now all variables are interpreted independently. The decoupled analyses leads to a neglecting of the coupled dependency of the real and imaginary parts. Hence, the solution becomes a little conservative. The conservatism grows with the value of the uncertainties in A and B polynomial.

To get a feeling of the magnitude by the overestimation, the influence of the parameter uncertainties of system $G_3(s)$ to the zeros of the function $h(\omega)$ is shown in Fig. 4. In this figure, the reference plot $h_{ref}(\omega)$ illustrates the course of $h(\omega)$ without parameter uncertainties. The plot $h_{\min}(\omega)/h_{\max}(\omega)$ illustrates the $h(\omega)$ function which leads to the smallest/greatest possible zeros by appropriate choice of the system parameters from their range of uncertainty. The amplitude offset (caused by ΔA and ΔB) seems very large, but with considering that the K_P values can no be bigger/smaller than $h_{\min}$ (Hohenbichler (2008)), the effect of this overestimation to the zeros of $h(\omega)$ is comparatively low. The effect of the frequency change created by the other system parameter (ΔA and ΔB - bounded by the arctan) is also relatively small. However, such generalizations are difficult because the resulting effect on the overestimation has a strongly dependency on the polynomials of the system transfer function. Fortunately, the conservatism is not critical because the undetected stable PID parameters are very close to the stability border and can easily lead to an instability.

One method to reduce the conservatism without losing the guarantee of robust stability of the whole resulting PID area is to use a numerical calculation of the rightmost eigenvalue of the system (e.g. using the DDB-BIFTOOL

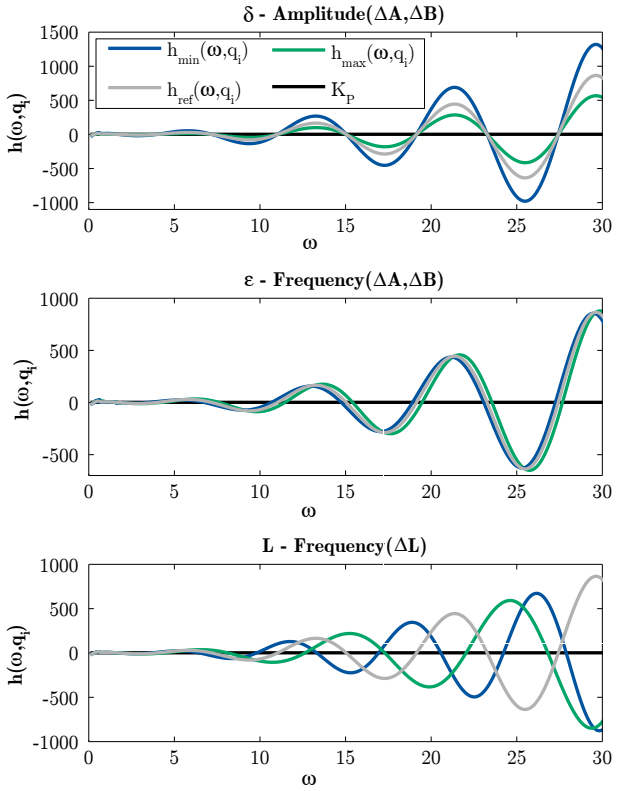

Fig. 4. Effect of the parameter uncertainties to $h(\omega, q_i)$

from Engelborghs et al. (2007)) in every corner of the previously calculated PID space. The PID space is limited by the root boundaries, where the closed system eigenvalue is zero (see section 2). Hence, the corners of the PID space can be adapted until the right most eigenvalue in each corner is equal to zero. The adaption can be realized as demonstrated by Michiels et al. (2002).

If a global optimization strategy is used, the starting values can be calculated iteratively. For a small K_P ($K_P \to 0$), equation (16) becomes very convenient. In this case, K_P and δ are going to zero. In the next step, the zeros of the sinus term must be found ($\lim_{\eta \to 0} \sin(\eta) = 0$). Hence, it only must be calculated when ϵ is equal to $\omega_{g,i} L$. The parameter set from which the optimized boundaries of $\omega_{g,i}$ are derived can be used iterative as starting point for the optimization of the next higher value of K_P.

When the min/max $\omega_{g,i}$ of each zero $\boldsymbol{\omega_g}$ interval is calculated, the corresponding min/max $K^0_{I,i}$ must be found. This can be done easily because L and ϵ only affect the frequency of the sinus term (see equation (15)). Hence, in the first step the amplitude α and the linear term γ is minimized/maximized like in section 3. In the second step, L and ϵ which min/max the individual $K^0_{I,i}$ are found using a simple parameter variations. Thereafter the resulting CRB bands mapped in the PID space, Fig. 5.

5. STABLE AREAS

The next task of the approach is to test which side of the root boundaries leads to a stable polygon. To realize this, in principle one PID parameter combination of each resulting 2D polygon (see e.g. the nine polygons in Fig. 5) can be taken to test the closed loop system stability (like in Engelborghs et al. (2007)) of all PID parameter convenient in the whole polygon. For a more comfortable methodology see Hohenbichler and Abel (2009). Fig. 5 b) illustrates a 2D subset of the PID parameter combinations of the system $G_3(s)$. In this example the polygon five leads to a stable closed loop system. Fig. 5 a) shows the PID space of $G_3(s)$ without parameter uncertainties. In the comparison of the two results it can be seen that the RRB does not change its shape. In the case of the CRBs, the single-lines transforms to bands. This has the consequence that the stability area A^* of b) gets smaller, caused of the parameter uncertainties. Most strongly increases the left boundary because the corresponding range of the third zero $\boldsymbol{\omega_g}$ interval is very large with consideration of the parameter uncertainties. This can be deduced from Fig. 3.

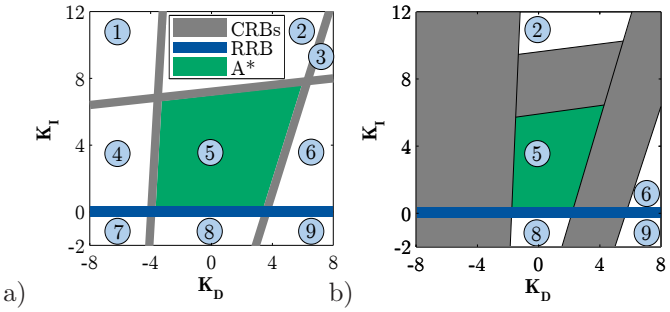

Fig. 5. Parameter areas: a)Robust approach b)Original

The introduced method provides the boundaries only for the K_I/K_D space on one fixed K_P. To add some K_I/K_D planes for several K_P values, only the CRBs must be updated (see equation (9)). Hence, the shape of the stable polygons can only change a bit and the computational effort is relatively low. To take into account the potential K_P-value range, the eligible K_P interval must be calculated. To do this, the algorithm from Hohenbichler (2008) is used. For each of the K_P values a new 2D plane results. At the end, of the calculation algorithm, a 3D polygon which shows all PID parameter combinations is created. To finish the parameter tuning method, one parameter combination of this 3D parameter space must be chosen.

6. PERFORMANCE REQUIREMENTS

The choice of problem specific PID parameters in the 3D parameter space sounds trivial. But in practice, it is difficult because it is hard to identify how the controller performance depends on the PID parameter location. One idea to solve this problem is parameter optimization. The goal of this method is that one optimization criteria can be selected (time/energy optimality in sens of LQR) and a parameter estimation algorithm computes the best PID parameter combination with respect to the borders of the stable PID space. On the one hand, for unexperienced users, the controller parameterization gets more easy because it is almost completely automatic and requires no detailed control theory knowledge. On the other hand for experienced users, a good starting value for the PID fine tuning (loop shaping or root locus method) results from this optimization. For benchmarking the performance of the system dynamics, the ideal step response is used. The optimization is done by MATLAB and ACADO (Houska

and Ferreau (2011)). ACADO provides powerful optimization algorithms and allows to set a lot of restrictions remain for the states (e.g. no overshoot) and the control value. The available parameter space can easily set to the optimizer, because the PID space is only limited by linear straight. Therefore the K_I/K_D parameter space can be divided, but each parameter space piece is always convex.

Another task is to find the PID-parameter combination that guarantees maximum robustness. As described previously, the RRB is constant, the IRB bands are increasing linearly and the CRBs are nonlinearly by variation of the system parameters and the time delay (see Fig. 5). So, it is not trivial to find the parameter combination of maximum robustness. During the application the area middle point (based on Weller (2008)) has been confirmed repeatedly as a good approach to achieve maximum robustness.

As mentioned before, one method for the controller fine tuning is the loop shaping of the frequency response. The idea of the loop shaping approach is that the user can set performance quality requirements in form of a sensitivity and complementary sensitivity function to the magnitude of the frequency response plot (in the sense of H_∞). Then an least square optimizer minimizes the deviation to the required frequency responses. The constraints like the 3D PID parameter space can be easily included in the optimizer and a piecewise convex (with precise knowledge of the convex area locations) optimization problem results.

A second method for the fine modification of the PID parameters is the root locus method. This method is extend to time delay systems by using a new branch and follow method, based on the root locus construction rules (Palm (1986)) of time delay systems.

7. CONCLUSION

The parameter space approach emerges as a convincing and easily understood method to compute the stable regions in the PID parameter spaces. An easy way to modify the parameter space approach to a one step procedure to guarantee robust stability was demonstrated. The presented approach explicitly considers uncertainties in the system parameters and time delay with only small conservatism. The challenging task of robust stability of time delay systems was converted to an easer minimum/maximum search to estimate the borders of the root boundary bands. To realize this, it must be calculated how the root boundaries change due the variation of system parameters. The transfer of the classic two step parameter space approach to a one step approach is achieved by the continuous consideration of the shift of the root boundaries with respect to the system parameter variation. To fix the drawback of the difficult choice of the most suitable PID parameters in the stable parameters space, several approaches for automatic criteria optimization and for additional controller fine tuning were briefly illustrated.

A major advantage for the industrial application of the proposed method is the great transparency and simplicity of the presented approach. The approach uses a very intuitive method and avoids completely more complex methods such as the Lyapunov stability. The whole methodology presented in this paper will be integrated in a MATLAB toolbox called PIDrobust. A preliminary version of the tools can be downloaded on the PIDrobust website http://www.irt.rwth-aachen.de/en/fuer-studierende/downloads/pidrobust.

Future work will deal with the improvement of the optimization strategies and the finalizing of the parameter tuning methods. Additionally, an extension of the controller classes (e.g. state feedback and sliding mode) is planned.

ACKNOWLEDGEMENTS

This work was supported by the German Research Foundation (DFG) as project AB 65/2-3. The grant is thankfully acknowledged.

REFERENCES

Ackermann, J. (2002). *Robust Control*. Springer.

Ebenbauer, C. and Allgöwer, F. (2006). Stability analysis for time-delay systems using rekasiuss substitution and sum of squares. *IEEE Conf. Decision Control, San Diego, CA*, 45, 53765381.

Engelborghs, K., Luzyanina, T., and Samaey, G. (2007). *DDE-BIFTOOL a Matlab package for bifurcation analysis of delay differential equations*. K.U.Leuven Department of Computer Science.

Fu, M., Olbrot, A.W., and Polis, M.P. (1989a). Introduction to the parametric approach to robust stability. *IEEE Control Systems Magazine*, 9, 7 – 11.

Fu, M., Olbrot, A.W., and Polis, M.P. (1989b). Robust stability for time-delay systems: the edge theorem and graphical tests. *IEEE Transactions on Automatic Control*, 34, 813 – 820.

Gu, K. and Niculescu, S.I. (2003). Survey on recent results in the stability and control of time-delay systems. *Journal of Dynamic Systems, Measurement, and Control*, 125, 158–165.

Hohenbichler, N. (2008). Calculating all KP admitting stability of a PID control loop. *Proceedings of the 17th IFAC World Congress*, 17, 5802–5807.

Hohenbichler, N. and Abel, D. (2009). All stabilizing PID controllers for time delay systems. *Automatica*, 45, 2678–2684.

Houska, B. and Ferreau, H.J. (2011). ACADO toolkit - an open-source framework for automatic control and dynamic optimization. *Optimal Control Methods and Application*, 32, 298–312.

Kharitonov, V.L. (1978). Asymptotic stability of an equilibrium position of a family of systems of differential equations. *Differentsialnye uravneniya*, 14, 2086–2088.

Michiels, W., Engelborghs, K., Vansevenant, P., and Roose, D. (2002). Continuous pole placement method for delay equations. *Automatica*, 38, 747–761.

Palm, W.J. (1986). *Control Systems Engineering*. John Wiley & Sons.

Walton, K. and Marshall, J. (1987). Direct method for TDS stability analysis. *Control Theory and Applications, IEEE Proceedings D*, 134, 101 – 107.

Weller, R.M. (2008). Automatisierter Entwurf von PID-Reglern mit dem Flächenschwerpunkt-Verfahren. Bachelor's thesis. Technische Universität München, Institute of Automatic Control Engineering.